AMERICAN JOURNAL OF PHARMTECH RESEARCH
Journal home page: http://www.ajptr.com/

Identification of Novel HDAC8 Inhibitors Using Pharmacophore Based Virtual Screening, 3D QSAR and Molecular Docking Approach

Sudhan Debnath[1*], Payel Nath[1], Ranendu Kumar Nath[2]
1. Department of Chemistry, MBB College, Agartala, Tripura, 799 004, India
2. Department of Chemistry, Tripura University, Suryamanninagar, Agartala, Tripura, India

ABSTRACT

In the present study a series of 20 histone deacetylase 8 (HDAC8) inhibitors were used for generation of pharmacophore. A five features pharmacophore with one hydrogen bond acceptor (A), two hydrogen bond donors (DD) and two ring aromatics (RR) was developed and used for searching compound database. A statistically significant atom based 3D QSAR model was built by selecting best pharmacophore hypothesis ADDRR.3 with R^2 = 0.9821 for training set of 14 molecules and Q^2= 0.7314, RMSE= 0.1709, Person-R= 0.9061 for test set of 6 molecules. These parameters indicate that the model is a good predictive model. Docking study of known inhibitors as well as hits resulted after data base searching having fitness score ≥ 1 was performed. Docking analysis shows the important residues in the active site of receptor are Zn-388, TYR-306, HIS-142, PHE-152, PHE-208, GLY-151, and HIE-180. The XP glide score of highest active compound **1** and lowest active 20 are -11.73 and -6.036 respectively, which corroborated with experimental activity. On the basis of pharmacophore matching, predicted activity and docking interactions 5 novel chemical scaffold (Code No: CACPD2011a-0001275680, CACPD2011a-0000573705, CACPD2011a-0001843791, CACPD2011a-0000300107, CACPD2011a-0000291783) are reported as potent HDAC8 inhibitors.

Keywords: Pharmacophore, Virtual screening, atom based 3D QSAR, HDAC8 inhibitors, Docking.

*Corresponding Author Email: bcsdebnath@gmail.com
Received 24 October 2014, Accepted 30 October 2014

Please cite this article in press as: Sudhan D *et al.*, Identification of Novel HDAC8 Inhibitors Using Pharmacophore Based Virtual Screening, 3D QSAR and Molecular Docking Approach. American Journal of PharmTech Research 2014.

INTRODUCTION

The enzymes Histone Acetyl Transferases (HATs) and Histone Deacetylases (HDACs) play important role in the acetylation and deacetylation of lysine residues of N-terminal region of core histones. Deacetylation of histones is associated with transcriptional repression, including a decrease in the expression of tumor suppressor genes [1]. Inconsistent with these observations, HDACs are over expressed in colon, breast, prostate, and other cancers making them a promising anticancer target. Inhibition of HDACs activities increase gene expression resulting in growth inhibition, differentiation, and apoptosis of cancer cells [2]. A large number of HDAC inhibitors have been isolated from natural products, or have been synthesized in laboratory. Among them a good number of HDAC inhibitors are in clinical trials as single agents for lymphoproliferative disorders and recently two of these agents, vorinostat and romidepsin, have been approved by FDA, USA for the treatment of relapsed and refractory cutaneous T cell lymphomas (CTCL) [3]. These facts encouraged the researchers for development of new HDAC inhibitors. HDAC 8 also differentially expressed and associated with various types of cancers. It is the only HDAC relevant in Neuroblastoma, [4] its inhibition induces apoptosis in T–cell cancers such as Leukamia [5,6]. Most of the HDACs inhibitors are from hydroxamic acid family. It shows strong chelation with Zn ion, due to this reason the hydroxamic acid could present metabolic and pharmacokinetic challenges [7]. Hence, inhibitors of non-hydroxamic acid group are the need of the hour. It is observed that most of the currently available HDAC inhibitors are unselective or inhibit either all or at least several members of the HDAC family. Therefore development of selective HDAC8 inhibitors may reduce the side effect. The objective of the present study is to develop pharmacophore hypothesis, virtual screening of chemical database by best pharmacophore and building of 3D QSAR model to predict the activity of hits as well as to know the detailed structural insight. Hits yielded from virtual screening subjected to glide docking to find out the more potent hits as HDAC8 inhibitors. Database screening, predicted activity of hits and docking study has come up with new scaffold which may be further designed and developed as more potential and selective inhibitors.

MATERIALS AND METHOD

Data Set

The compounds with IC_{50} value were collected from the literature [8] which comprised of 20 HDAC8 inhibitors from same assay series. The IC_{50} values were converted to pIC_{50} by taking negative logarithm to base 10 of IC_{50} and the range of pIC_{50} values were 4.456 – 8.097 (Table 1). The dataset was randomly divided into training set (70%) and test set (remaining 30%). The X-ray

crystal structures of HDAC8 were collected from RCSB protein data bank (PDB ID: 1T64) for docking study. All the computational work was carried out by using HP Z820 Workstation running over CentOS 6.3.

Table 1: Data set with actual activities, predicted activities and fitness score

Compound No	QSAR Set	Activity	Factors	Predicted Activity	Pharm Set	Fitness
01	training	8.097	2	8.08	active	3.00
02	training	7.658	2	7.71	active	1.38
03	training	6.921	2	6.94	active	1.90
04	training	6.793	2	6.59		1.69
05	training	6.721	2	6.77		1.48
06	training	6.538	2	6.58		2.26
07	test	6.45	2	6.50		0.99
08	training	6.284	2	6.33		0.83
09	test	6.27	2	6.38		0.95
10	training	6.221	2	5.98		1.02
11	test	6.161	2	6.04		1.36
12	training	6.086	2	6.04		1.19
13	test	6.073	2	6.26		1.05
14	training	5.998	2	6.08		1.64
15	test	5.971	2	5.95		1.43
16	training	5.41	2	5.48		1.21
17	test	5.398	2	5.73		1.21
18	training	5.013	2	5.11	inactive	1.38
19	training	4.658	2	4.94	inactive	1.43
20	training	4.456	2	4.24	inactive	1.31

Ligand Preparation

The first step for pharmacophore generation was ligand preparation. All the structures were drawn using maestro 2D sketcher then converted the structures into 3D and then saved as .mae format then imported in Maestro 9.6 interface. After that ligand preparation was done using LigPrep module of Schrödinger. A single, low energy, 3D structure with retained chiralities and keeping original state of ionization was prepared during ligand preparation of each input structure.

Protein Preparation and Receptor Grid Generation

The receptor 1T64 was prepared through preprocessed, optimized and minimized with OPLS_2005 force field using Protein Preparation Wizard. The Grid were generated selecting the centroid of the workspace co-ligands of the prepared proteins using the Receptor Grid Generation panel of Schrodinger with default options unless stated otherwise. The ligand was selected to define the position and size of the active site during grid generation. The RMSD of 1T64 was calculated by superimposing XP-Glide generated best docked conformation on its original X-ray

crystallographic bound conformation and the value was 0.30Å. This RMSD value indicated that glide was able to reproduce the native conformation successfully and the generated receptor grid of 1T64 could be used for docking and virtual screening.

Pharmacophore Identification

PHASE [9,10] has standard set of six pharmacophore features, hydrogen bond acceptor (A), hydrogen bond donor (D), hydrophobic group (H), negatively ionizable (N), positively ionizable (P), and aromatic ring (R). Common pharmacophoric sites were created by default features. The variants were generated with maximum five sites which were matched with two active ligands. It gave five hypotheses (Table 2) which were scored on the basis of alignment on active ligand. The maximum RMSD value was 1.2 Å for distance tolerance, keeping with vector score, volume score, and site score were 1.0. The quality of alignment was calculated by survival score and survival minus inactive score [11, 12]. The survival score and survival-inactive score of hypothesis ADDRR.3 was highest (Figure 1) and used for virtual screening and 3D QSAR model building.

Table 2: Pharmacophore Hypothesis according to scoring values

ID	Survival	Survival -inactive	Post-hoc	Matches
AADRR.1	4.378	3.19	2.896	2
AADRR.3	4.378	3.19	2.896	2
ADDRR.3	**4.586**	**3.212**	**2.904**	**2**
DDRR.12	4.171	2.898	2.355	2
DDRR.10	4.133	2.967	2.355	2

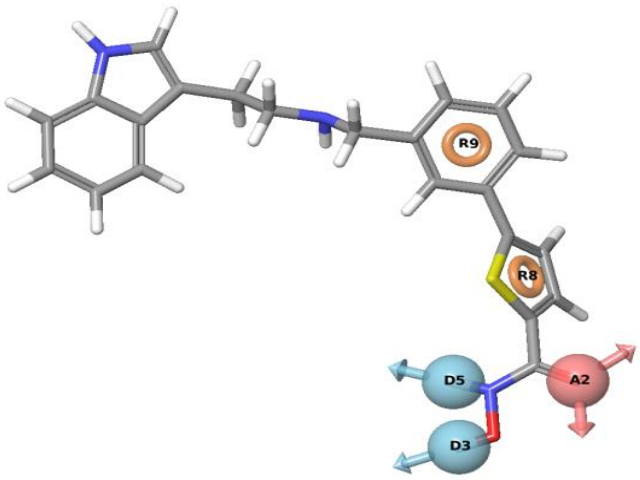

Figure 1: Phase generated Pharmacophore model ADDRR.3 of most active ligand illustrating hydrogen bond acceptor (A: pink), hydrogen bond donor (D: sky) and aromatic ring (R: orange) features.3D QSAR Model

PHASE provides the build QSAR option and the hypothesis ADDRR.3 was selected for 3D QSAR model generation. During model building randomly selected training set was kept as 70% and

atom based model was generated by keeping 1Å grid spacing and 2 as maximum number of PLS factors.

Virtual Screening of Database

Phase database was used for virtual screening to find out the potential HDAC8 inhibitors and the workflow of which was shown in Figure 2. The Phase database [Phase CAC (Commercially Available Compounds) database was prepared by SD files of commercially available compounds were obtained from the following vendors: Asinex (www.asinex.com), Bionet(Key Organics) (www.keyorganics.ltd.uk), ChemDiv (chemdiv.emolecules.com), Enamine (www.enamine.net), LifeChem (www.lifechemicals.com), Maybridge (www.maybridge.com), Specs (www.specs.net), TimTec (www.timtec.net)] containing 4.3 x 10^6 molecules (only first conformer) of previously prepared, with unique identifier code: CACPD2011a compounds. The database ligands were fully prepared previously in such a way that there were no duplicate, protonated in appropriate protonation states, skipping structures with reactive functional groups, posses possible least energy conformations and retained drug like molecules only using Phase.

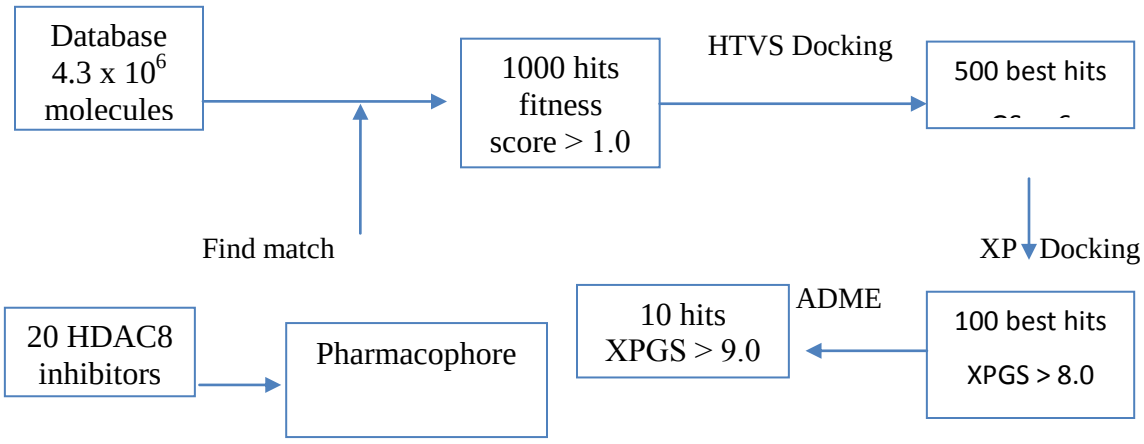

Figure 2: Workflow for identification of novel HDAC8 inhibitors

Docking Study

Molecular docking study of 20 known inhibitors was performed with receptor gird of 1T64 to know the active site residue interactions. Docking study of 1000 hits resulted after pharmacophore based database screening was also carried out with same receptor gird to investigate the best ligands binding affinity using GLIDE [13, 14, 15, 16]. Firstly high throughput virtual screening (HTVS) was carried out for all the hits. Then 50% of the best hits yielded after HTVS subjected for glide extra precision (XP) docking (Figure 2).

Model Validation

The prediction ability of a model is evaluated by a well-known ‘‘leave-one-out’’ (LOO) cross-validation [17] method. Usually internal validation of a model built from training set is satisfactory to confirm its predictive power. But a high R^2 (≥ 0.70) shows a good internal validation for training set only [18]. A good internal validation does not conclude its good predictive ability for an external test set [19]. Therefore for reliable predictive model external validation is also essential. For external validation RMSE (Root-mean-square error), Q^2 (test set correlation), and Pearson-R (between the predicted and observed activity for the test set) were used. For good predictive model RMSE values should be low < 0.30, $Q^2 > 0.60$ [18] and Pearson-R should be > 0.8. The other criteria for a good model are R^2–Q^2 should not be more than 0.3 [20], SD (standard deviation) should be small, highest F value highest and lowest P value containing factor should be considered.

RESULTS AND DISCUSSION

Five features pharmacophore hypotheses ADDRR.3 gave a statistically significant atom based 3D QSAR model having regression coefficient R^2: 0.9821, SD: 0.1534, Q^2: 0.7314, RMSE: 0.1709, Pearson-R: 0.9061. Results of QSAR model with PLS 2 of ADDRR.3 hypothesis are presented in Table 3. The correlation between predicted and experimental activities of training set and test set molecules are presented in Figure 3. All the statistical parameters are delete lie in the recommended range and hence the model is was statistically significant and predictive.

Table 3: Statistical parameters for the best pharmacophore hypotheses

ID	Factors	SD	R-squared	F	P	Stability	RMSE	Q-squared	Pearson-R
ADDRR.3	1	0.3392	0.9047	114	1.761e-07	0.0396	0.2054	0.6122	0.8587
	2	0.1534	0.9821	302.4	2.43E-10	0.0153	0.1709	0.7314	0.9061

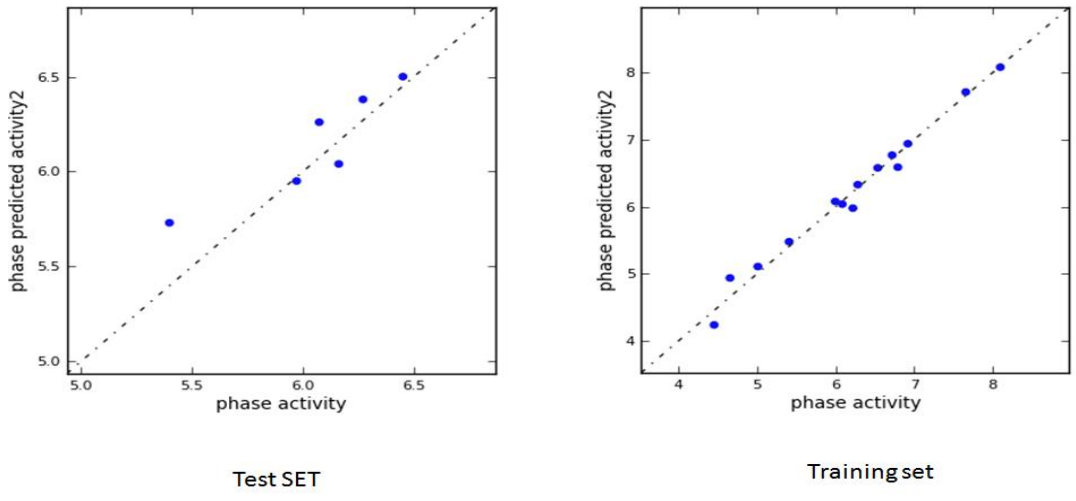

Figure 3: Fitness graph between observed activity and Phase predicted activity for training and test set compounds.

3D QSAR Analysis

The structural insight into HDAC8 inhibitory activity was observed by visualizing 3D QSAR model. This visualization information's could be used for development of potent HDAC8 inhibitors. The model was applied to the most active compound **1** and the least active compound **20** and are were shown in the Figure 4,5,6.

Hydrogen bond Donor

Analysis of 3D QSAR visualization generated by PHASE suggested that blue cube region were favorable for introduction of hydrogen bond donor group and the orange cubes regions indicates that these positions should not be occupied by hydrogen bond donor group for better HDAC8 inhibitory activity (Figure 4).

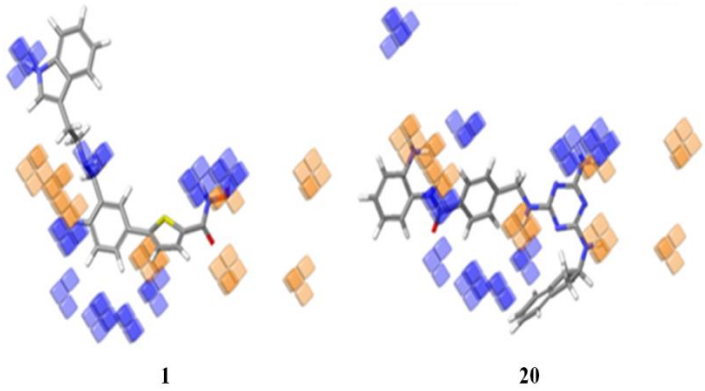

Figure 4: Hydrogen bond donor visual representation of 3D QSAR model of 1 and 20 (Blue cubes indicate favorable regions while orange cubes indicate unfavorable region).

Hydrophobic Interaction

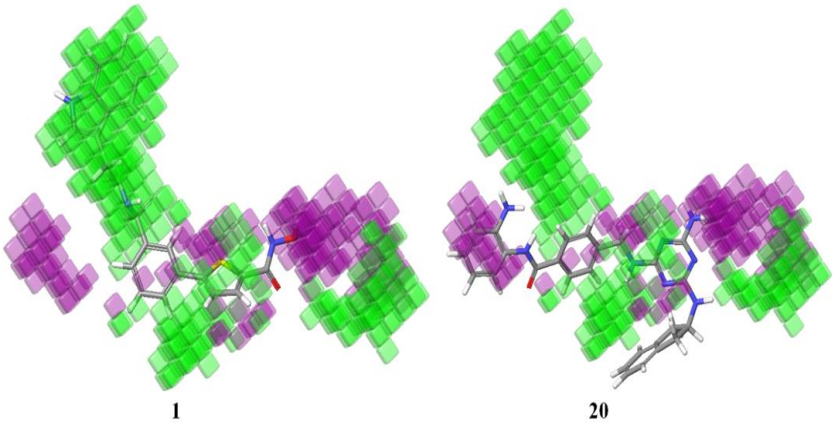

Figure 5: Hydrophobic visual representation of 3D QSAR model of 1 and 20 (Green cubes indicate favorable regions while purple cubes indicate unfavorable region for activity).

3D QSAR visualization of hydrophobic interaction (Figure 5) on both highest active **1** and lowest active **20** ligand generated by Phase suggested that the green cubes indicate favorable regions for

hydrophobic interaction and the purple cubes indicate regions that are unfavorable for hydrophobic interaction for better HDAC8 inhibitory activity.

Electron Withdrawing Effect

The blue regions appeared in pictorial presentation (Figure 6) for electron withdrawing effect around the highest active **1** and lowest active ligand **20** indicates that introduction of electron withdrawing group in this region will favour the HDAC8 inhibitory activity and the red cube region around the ligands indicate that it is is unfavorable for substitution with electron withdrawing groups.

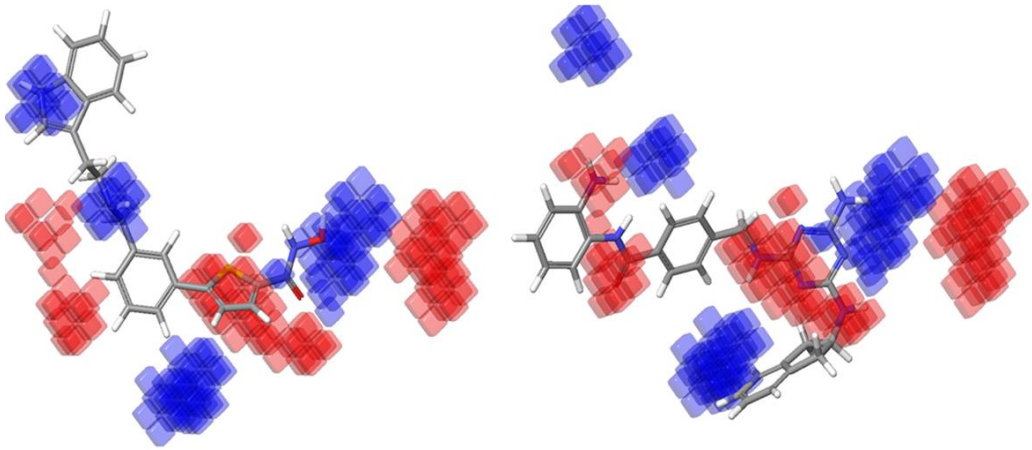

Figure 6: Electron withdrawing visual representation of 3D QSAR model of compound 1 and 20 (Blue cubes indicate favorable regions while red cubes indicate unfavorable region for the activity)

Docking Analysis

The docking analysis shows that most of the inhibitors interacts with Zn-388 (18, Zn…O=C; 8, Zn…OH) (number of interactions was shown in the parenthesis). The other key interacting amino acid residues are were TYR-306 (10), HIS-142 (8), PHE-152 (11), PHE-208 (7), GLY-151 (6), HIE-180 (4). The other less interacting amino acid residues are were TYR-100 (3), HIS-143 (2), PHE-207 (2). Therefore, if identified hits interact with active site amino acid residues like inhibitors then those hits may have greater binding affinity with receptors. Among the five hits four interacts with Zn (3, Zn…O=C; 1, Zn…OH) and the other interacting amino acid residues are were TYR-306 (4), PHE-152 (9), GLY-151 (2), TYR-100 (2). All the identified hits interact with active site of HDAC8 similar to inhibitors. The 2D ligand interaction diagram of known inhibitors and five hits are presented in Table 4 and Table 5 respectively. The XP glide score of highest active and lowest active molecules 1, 2, 19, 20 are were -11.73, -10.09, -8.21,-6.036 respectively, which corroborate d with experimental activity. The summary of interactions of both inhibitors and

hits are presented in Table 6. Five structurally diverse potent inhibitors identified form 500 hits having high binding affinity and interactions with Zn are reported as HDAC8 inhibitors.

Table 4: Structure of Inhibitors, Type of Interactions of Inhibitors with Active Site Residues: HBD (Hydrogen Bond Donor), HBA (Hydrogen Bond Acceptor), Π-Π Interactions, Zn (Interacting Distance), XP-Glide Score (XPGS)

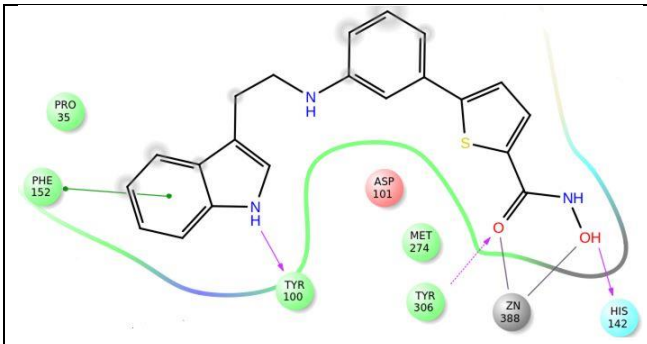 **1**	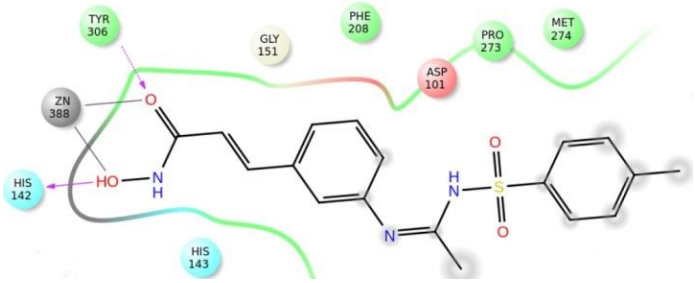 **2**
HBD= HIS-142, TYR-100; HBA= TYR-306; Π-Π= PHE-152; Zn...O=C 2.12 Å, Zn...OH 2.24 A°; XPGS: -11.730	HBD= HIS-142; HBA= TYR-306; Zn...O=C 2.22 Å Zn...OH 2.23 Å ; XPGS: -10.091
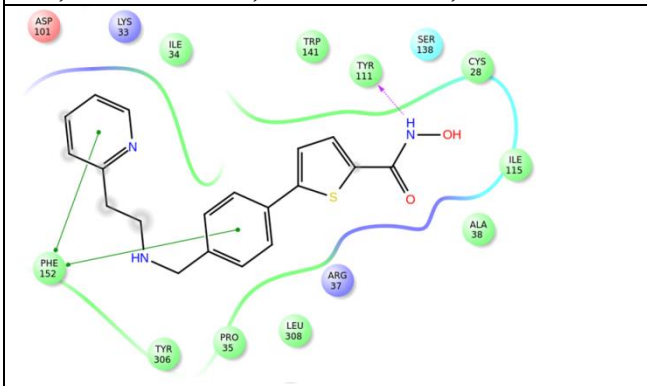 **3**	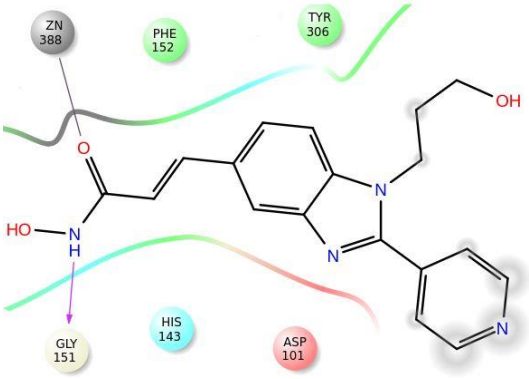 **4**
HBD= TYR-111; Π-Π= PHE-152 (2); Zn...O=C 2.12 Å, Zn...OH 2.24 A°; XPGS: -9.107	HBD= GLY-151; Zn...O=C 2.09 Å, XPGS: -8.706
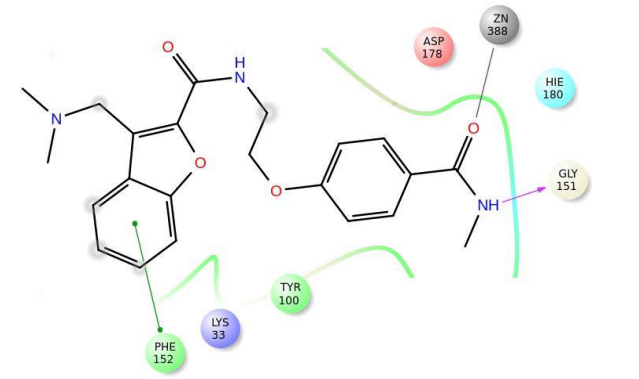 **5**	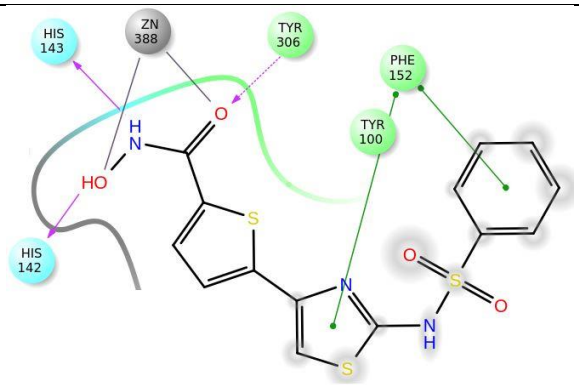 **6**
HBD= GLY-151; Π-Π= PHE-152; Zn...O=C 2.02 Å; XPGS: -10.552	HBD= HIS-142, HIS-143; Π-Π= PHE-152 (2); HBA= TYR 306; Zn...O=C 2.16 Å; Zn…OH 2.25 Å; XPGS: - 8.784

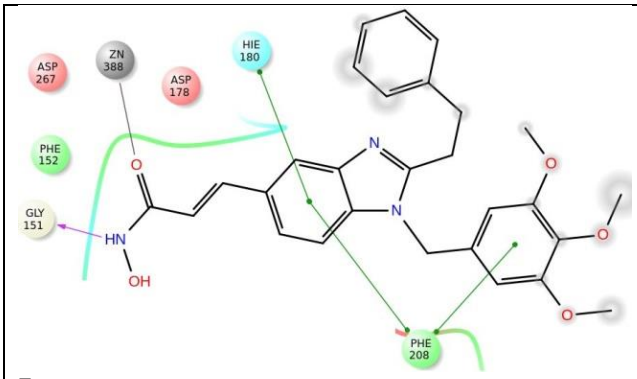

7

HBD= GLY-151; Π-Π= PHE-208(2), HIE-180
Zn...O=C 2.07 Å; XPGS: -9.385

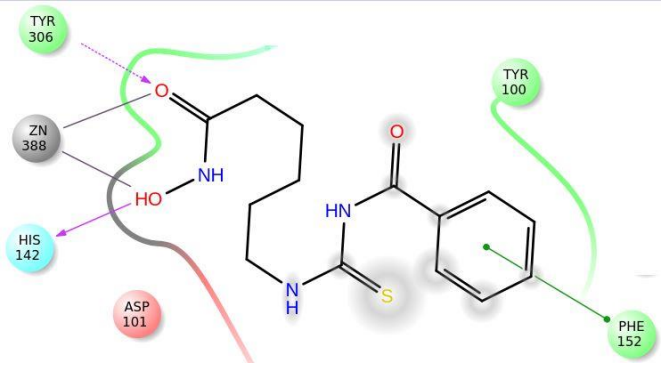

8

HBD= HIS-142; HBA= TYR-306; Π-Π= PHE-152
Zn...O=C 2.30 Å, Zn...OH 2.23 Å; XPGS: -8.801

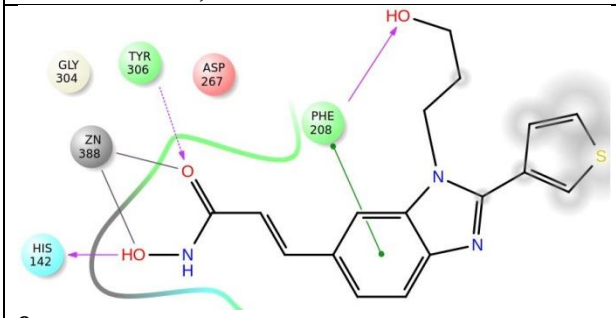

9

HBD= HIS-142; HBA= TYR-306, PHE-208; Π-Π= PHE-208; Zn...O=C 2.24 Å Zn...OH 2.23 Å; XPGS: -8.421

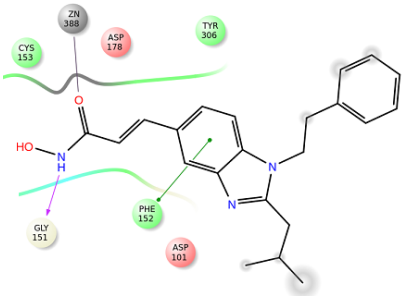

10

HBD= GLY-151; Π-Π= PHE-152; Zn...O=C 2.09 Å;
XPGS: -8.359

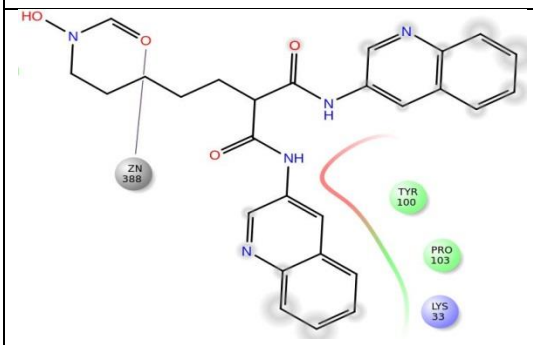

11

Zn...O=C 2.09 Å; XPGS: -8.779

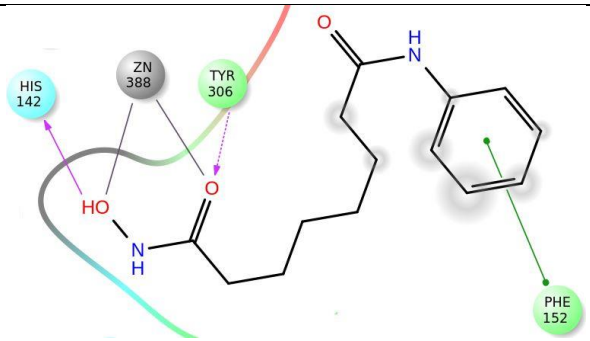

12

HBD= HIS-142; HBA= TYR-306; Π-Π= PHE-152
Zn...O=C 2.31 Å, Zn...OH 2.23 Å; XPGS: -8.973

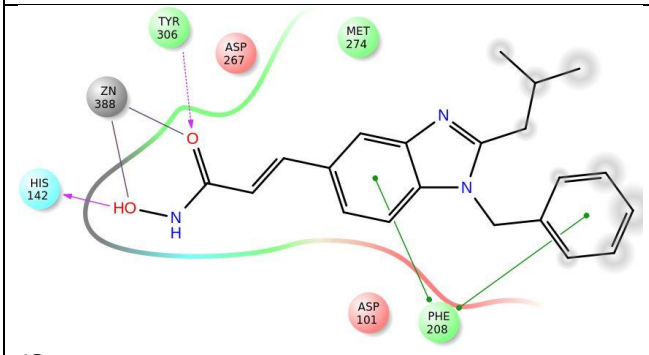

13

HBD= HIS-142; HBA= TYR-306; Π-Π= PHE-208 (2);
Zn...O=C 2.26 Å; Zn...OH 2.23 Å; XPGS: -8.637

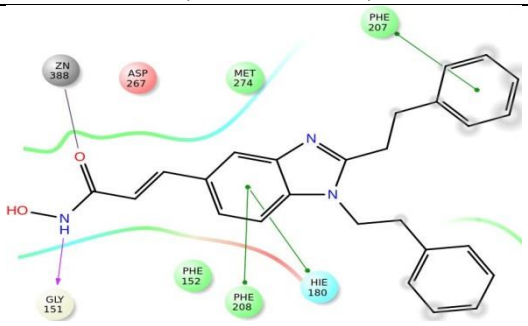

14

HBD= GLY-151; Π-Π= PHE-208, HIE-180, PHE-207;
Zn...O=C 2.02 Å, XPGS: -9.227

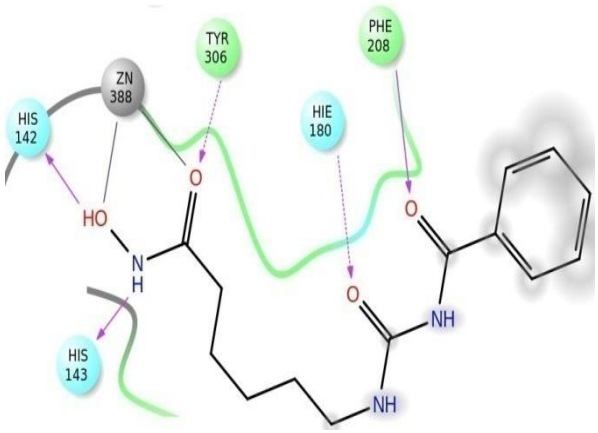 **15**	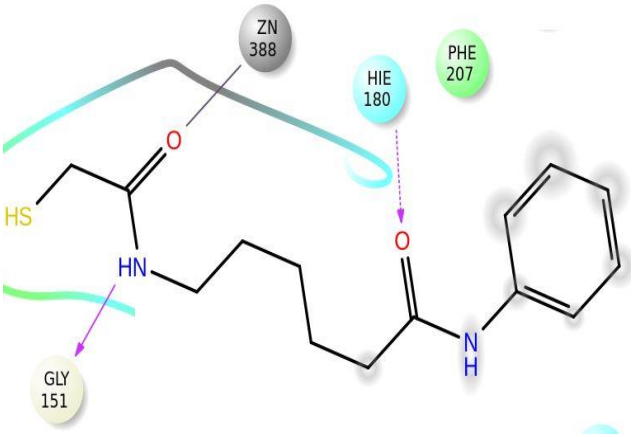 **16**
HBD= HIS-143, HIS-142; HBA= TYR-306, HIE-180, PHE-208; Zn...O=C 2.27 Å, Zn...OH 2.24 Å, XPGS: -9.301	HBD= GLY-151; HBA= HIE-180; Zn...O=C 2.11 Å, XPGS: -8.476
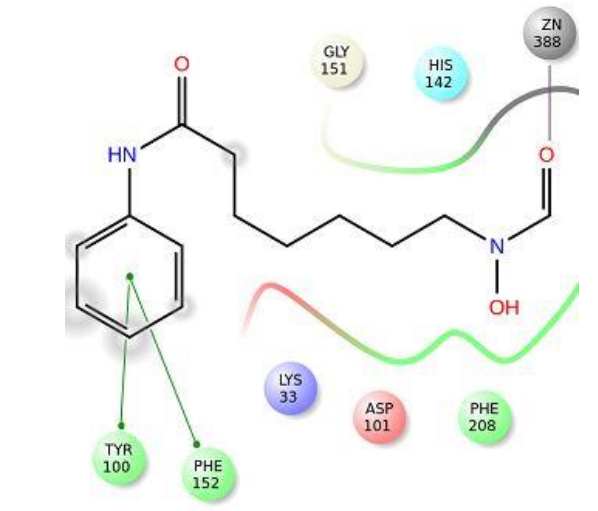	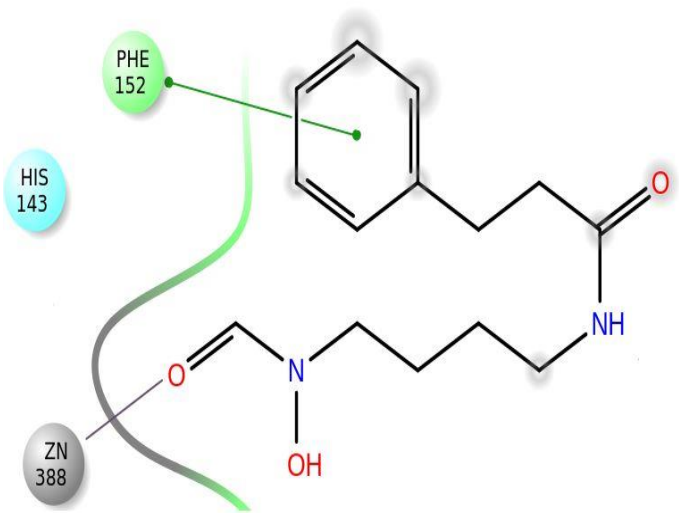 **18**
Π-Π= PHE-152, TYR-100; Zn...O=C 2.09 Å; XPGS: -8.212	Π-Π= PHE-152; Zn...O=C 2.09 Å, XPGS: -8.277
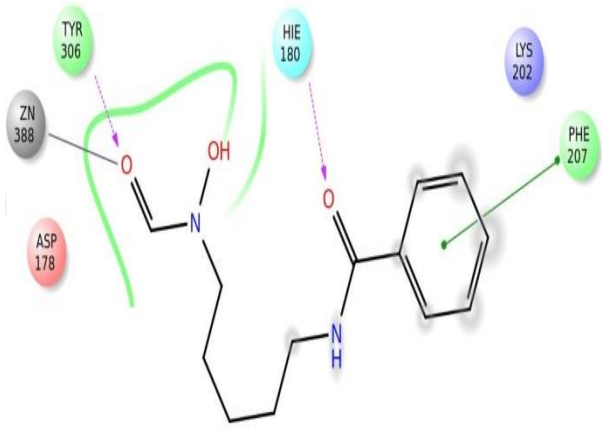 **19**	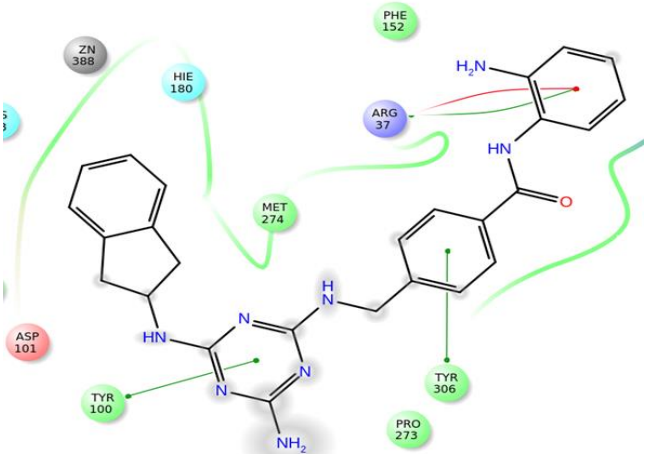 **20**
HBA= TYR-306, HIE-180; Π-Π= PHE-207; Zn...O=C 2.03Å; XPGS: -8.213	Π-Π= TYR-100, TYR-306, ARG-37 (2); XPGS: -6.036

Table 5: Structure of ptential Hits, Type of Interactions: HBD (Hydorgen Bond Donor), HBA (Hydrogen Bond Acceptor), π-π interactions, Zn (Interaction Distance) XP Glide Score (XPGS), Predicted Activity (PA), Fitness Score (FS)

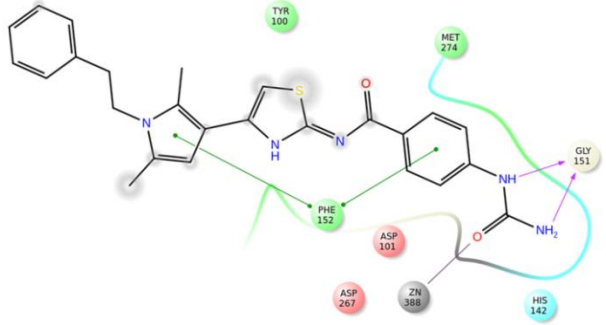 **CACPD2011a-0001275680**	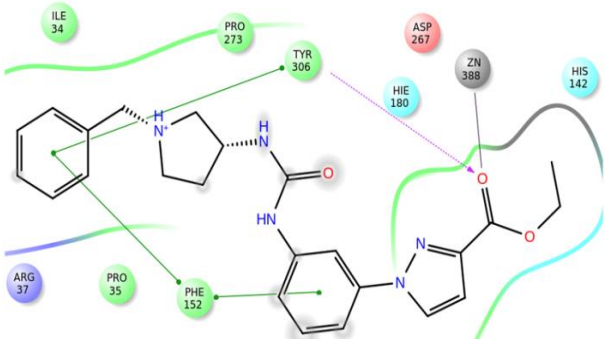 **ACPD2011a-0000573705**
HBD= –NH…GLY-151(1.88 Å); -$CONH_2$...GLY-151 (2.36 Å); Π-Π= PHE-152 (2); >C=O…Zn (2.05 Å); XPGS = – 9.594. PA: 6.884; FS: 1.9033	HBA= >C=O…TYR 306 (1.94 Å); Π-Π= PHE-152 (2), TYR-306; >C=O…Zn (2.28 Å); XPGS = –9.103. PA: 6.3074; FS: 1.8572
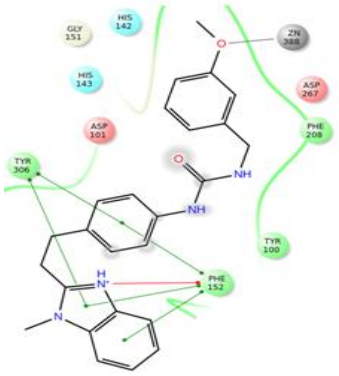 **CACPD2011a-0001843791**	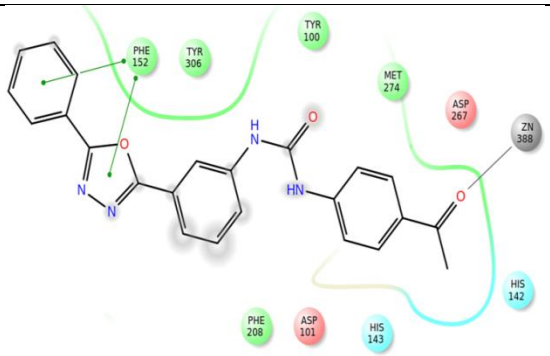 **CACPD2011a-0000300107**
Π-Π= PHE-152(3),TYR-306 (2); π-cation = PHE-152; Ph–O…Zn (2.25 Å); XP GS = –8.538; PA: 6.48; FS: 1.8529	Π-Π= PHE-152 (2); >C=O…Zn (2.11); XP GS =–7.587; PA: 5.7393; FS: 1.8557
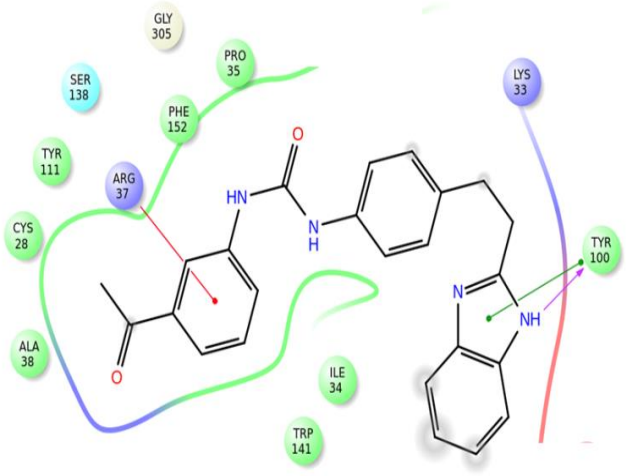 **CACPD2011a-0000291783**	
Π-Π=TYR-100; π-cation = ARG-37; HBD= TYR-100 (2.02 Å) ; XPGS= –8.733; PA: 6.2910; FS: 1.8614	

Table 6: Type and Number of Hydrophobic (Π-Π), Hydrogen Bond Donor (HBD), Hydrogen Bond Acceptor (HBA), Metal (Zn) of 20 inhibitors and 5 identified inhibitors

Number of Interactions for 30 known inhibitors						Number of Interactions for newly identified 5 inhibitors				
Residues	Π-Π	HBD	HBA	Zn….0=C	Zn….O-H	Π-Π	HBD	HBA	Zn….0=C	Zn….O
TYR-306	1		9			3		1		
HIS-142		8								
TYR-100	2	1				1	1			
HIS-143		2								
GLY-151		6					2			
HIE-180	2		2							
PHE-208	5		2							
PHE-207	2									
PHE-152	11					9				
Zn-388				18	8				3	1

CONCLUSION

Hypothesis ADDRR.3 generated the best pharmacophore model which was used for virtual screening of 3D database. Database searching identified 1000 hits having fitness score > 1.0. A statistically significant atom based 3D QSAR model was built by selecting best pharmacophore hypothesis ADDRR.3 with R^2 = 0.9685, SD= 0.1442, F= 205.2, Q^2 = 0.7119, Pearson R = 0.8727 and activity of hits predicted by this model. The XP glide score of highest active and lowest active inhibitors corroborated with the experimental activities of inhibitors. Therefore the docking information of known inhibitors compared with docking information of hits yielded after virtual screening may also considered for identification of potent molecules. On the basis of pharmacophore matching, predicted activity, docking analysis five novel scaffolds as potential HDAC8 inhibitors with unique code are reported in the paper. All the identified inhibitors are from non-hydroxamate family. The result of pharmacophore hypothesis, atom based 3D QSAR model give detailed structural insights as well as highlights important binding features also. Using above information the selected hits may be further developed as selective and more potential inhibitors which may likely reduce time, effective cost and the number of HDAC8 inhibitor to be synthesized.

ACKNOWLEDGEMENTS

The authors are thankful to Department of Biotechnology, New Delhi, Govt. of India for providing financial support [F.No.BT/327/NE/TBP/2012] for this research work.

REFERENCES

1. Bolden JE, Peart MJ, Johnstone RW. Anticancer activities of histone deacetylase inhibitors, Nat Rev Drug Discov 2006; 5: 769-84.
2. Carew JS, Giles FJ, Nawrocki ST. Histone deacetylase inhibitors: mechanisms of cell death and promise in combination cancer therapy. Cancer Lett 2008; 269:7-17.
3. Zain J, O'Connor OA.Targeting histone deacetyalses in the treatment of B- and T-cell malignancies. Invest New Drugs 2010; Suppl 1: S58-78.
4. Oehme I, Deubzer HE, Wegener D, Pickert D, Linke JP, Hero B et al, Histone deacetylase 8 in neuroblastoma tumorigenesis. Clin Cancer Res 2009; 15: 91-9.
5. Gryder BE, Sodji QH, Oyelere AK. Targeted cancer therapy: giving histone deacetylase inhibitors all they need to succeed. Future Med Chem 2012; 4:505-24.
6. Balasubramanian S, Ramos J, Luo W, Sirisawad M, Verner E, Buggy JJ. A novel histone deacetylase 8 (HDAC8)-specific inhibitor PCI-34051 induces apoptosis in T-cell lymphomas. Leukemia 2008; 22:1026-34.
7. Patil V, Sodji QH, Kornacki JR, Mrksich M, Oyelere AK. 3-Hydroxypyridin-2-thione as novel zinc binding group for selective histone deacetylase inhibition. J Med Chem 2013; 56: 3492-506.
8. Thangapandian S, John S, Sakkiah S, Lee KW. Docking-enabled pharmacophore model for histone deacetylase 8 inhibitors and its application in anti-cancer drug discovery. J Mol Graph Model 2010; 29: 382-95.
9. Phase, version 3.4, Schrödinger, LLC, New York, NY, 2012.
10. Dixon SL, Smondyrev AM, Knoll EH, Rao SN, Shaw DE, Friesner RA. PHASE: a new engine for pharmacophore perception, 3D QSAR model development, and 3D database screening: 1. Methodology and preliminary results. J Comput Aided Mol Des 2006; 20: 647-71.
11. Boyd DB, Successes of computer-assisted molecular design, In Lipkowitz, Reviews in computational chemistry. VCH, New York, 1990; 355–371.
12. Tawari NR, Bag S, Degani MS. Pharmacophore mapping of a series of pyrrolopyrimidines, indolopyrimidines and their congeners as multidrug-resistance-associated protein (MRP1) modulators. J Mol Model 2008; 14: 911-21.
13. Glide, version 6.0, Schrödinger, LLC, New York, NY, 2013

14. Friesner RA, Banks JL, Murphy RB, Halgren TA, Klicic JJ, Mainz DT et al. Glide: a new approach for rapid, accurate docking and scoring. 1. Method and assessment of docking accuracy. J Med Chem 2004; 47:1739-49.
15. Halgren TA, Murphy RB, Friesner RA, Beard HS, Frye LL, Pollard WT et al. Glide: a new approach for rapid, accurate docking and scoring. 2. Enrichment factors in database screening. J Med Chem 2004; 47:1750-9.
16. Friesner RA, Murphy RB, Repasky MP, Frye LL, Greenwood JR, Halgren TA et al. Extra precision glide: docking and scoring incorporating a model of hydrophobic enclosure for protein-ligand complexes. J Med Chem 2006; 49: 6177-96.
17. Tetko IV, Tanchuk VY, Villa AE. Prediction of n-octanol/water partition coefficients from PHYSPROP database using artificial neural networks and E-state indices. J Chem Inf Comput Sci 2001; 4:1407-21.
18. Veerasamy R, Rajak H, Jain A, Sivadasan S, Varghese CP, Agrawal RK. Validation of QSAR Models-Strategies and Importance. Int J Drug Des & Disc 2011; 2: 511-19
19. Roy DR, Sarkar U, Chattaraj PK, Mitra A, Padmanabhan J, Parthasarathi R et al. Mol Divers 2006; 10: 119-131
20. Leach AR. Molecular modeling: Principles and applications. United Kingdom, Pearson Education Ltd. 2001